Journal of the European Ceramic Society 17 (1997) 1579–1586

PII: S0955-2219(97)00032-0
0955-2219/97/$17.00

Dynamic Fatigue Behavior of Two SiC and a SiCp Reinforced Al_2O_3 at Elevated Temperatures

Kristin Breder & Victor J. Tennery

Metals and Ceramics Division, Oak Ridge National Laboratory, Oak Ridge, TN 37831-6069, USA

(Received 2 October 1995; revised version received 18 July 1996; accepted 3 February 1997)

Abstract

Dynamic fatigue behavior of a siliconized SiC, a sintered β-SiC, and a SiCp (silicon carbide particle)-reinforced Al_2O_3 formed by directed oxidation of Al metal, which are considered for use in heat exchangers in coal-fired power plants, were evaluated at 1100 and 1400°C in air. Four-point flexure specimens were tested at five stressing rates from 37 MPa s^{-1} to 0·0001 MPa s^{-1} resulting in total times to failure up to 1200 h. Thirty specimens of each material were tested at the fast-fracture condition and 10 specimens were tested at the four dynamic fatigue conditions at each temperature. At 1100°C none of the materials exhibited any loss of strength as a function of stressing rate and very little tendency to creep was observed. At 1400°C the sintered β-SiC exhibited no strength loss, while the siliconized SiC showed a significant loss of strength and some signs of creep at stressing rates less than 0·01 MPa s^{-1}. The SiCp reinforced Al_2O_3 exhibited extensive creep at stressing rates ranging from 0·01 to 0·0001 MPa s^{-1} at 1400°C, in fact at the slower stressing rates the creep was dominant and the specimens could not be brought to fracture in the four point flexure fixtures. Extensive fractography showed that the failure mode for the sintered β-SiC was indeed a fast-fracture mode at all temperatures and stressing rates, the specimens mostly failing from pores in the microstructure. The siliconized SiC failed partly from pores and partly from metal inclusions at 1100°C and fast stressing rates, and at 1400°C at slower stressing rates slow crack growth was observed to occur with the Si-metal inclusions as starting points. The failure modes in SiCp reinforced Al_2O_3 changed from fast fracture from residual Al-alloy rich areas to a creep failure at intermediate stressing rates at 1400°C. © 1997 Elsevier Science Limited.

1 Introduction

In order for the United States to be able to continue to use coal as a major energy source in electricity production, future coal-fired systems must have minimal environmental impact and operate at much higher thermal efficiencies than the present systems. These systems must have low emissions of NO_X, SO_X and particulates, and will have lower CO_2 emissions due to a higher thermal efficiency of the overall power generation cycle. Significant improvements in efficiency compared to current systems will require a change to gas turbines (Brayton Cycle) instead of exclusive reliance on steam turbines (Rankine Cycle). In order to maximize efficiency, the working fluid at the turbine inlet must be at the highest possible temperature relative to ambient. Furthermore, to minimize corrosion and erosion of the stators and rotors in the turbine, it is preferable that air rather than combustion products be used for the working fluid. This can be achieved through the use of ceramic heat exchangers which can operate at temperatures up to 1600°C.[1–4]

The concept of ceramic heat exchangers, for use in externally fired combined cycles (EFCCs) for power generation, has been evaluated over several years. Much work was conducted in the late 1970s and early 1980s to conceptualize the design, test materials, and build prototypes.[5,6] Several materials were tested in combustion environments, and in some environments SiC survived quite well.[7–14]

The leading candidate materials for high-temperature pressurized heat exchanger application are still SiC-based ceramics, due to their potentially low cost and demonstrated fabrication technology relative to alternate refractory materials. Considerable improvement in the properties of these

materials has been achieved, to the point that they are reaching maturity as engineering materials. Some high-temperature mechanical property data for clean environments are available; however, the amount of long-time data for creep and slow-crack growth (SCG) is limited. In addition to the sintered and siliconized SiC materials, other materials have recently been proposed. A relatively new SiC particulate-reinforced Al_2O_3 ceramic has emerged as another candidate for this application,[15] but except for some creep results, there is very little long-term data available.[16] This particulate-reinforced material is produced by directed oxidation of molten metal containing the reinforcing phase, and the resulting composite contains some residual Al-metal ($\approx 13\%$) and porosity. The phase composition can be tailored to specific mechanical requirements. The thermal shock properties, as well as the thermal conductivity, are good for this type of material. Initial results further indicate that the composite has good corrosion resistance both in a coal slag environment and in sodium silicates.[17–19]

The high-temperature mechanical properties of sintered and siliconized SiC have been reported by many authors.[20–35] However, these materials have been under continuous development for many years, and several of the earlier reports describe materials with properties inferior to today's materials having essentially the same names. Work by Trantina and Johnson[20] and Evans and Lange[21] on sintered SiC with boron as the sintering aid showed promising mechanical properties up to 1400°C. It was found that sintered SiC had essentially no SCG in air, measured by double torsion (DT) or dynamic fatigue, at 1550°C. The siliconized and hot-pressed SiC exhibited some SCG, with crack velocity exponents, n, ranging from 20 to 50.[20,21] Quinn and Katz[22] performed stepped-temperature stress-rupture tests on sintered α-SiC at 1000 to 1400°C. At 1200°C they reported a time-dependent failure which would be typical of SCG behavior with $n=40$. However, there was no fractographic evidence of SCG, and the observed strength degradation was attributed to oxidation of surface connected porosity. They also indicated that this behavior would not be observed in specimens with artificially induced flaws (indentation or DT) because these specimen types failed at stress levels which were not high enough to cause stress corrosion. The specimens stepped up to 1400°C showed fractographic evidence of SCG. McHenry and Tressler tested hot-pressed SiC and sintered α-SiC.[23,24] They found no SCG for α-SiC at low oxygen partial pressures, but after oxidizing the specimens in air at 1200°C for 15 h, SCG was observed in both materials. Easler, *et al.*[25] evaluated the room-temperature fast-fracture strength after oxidizing α-SiC and hot-pressed SiC (NC203) with and without mechanical stress. More severe oxidation and subsequent weakening were reported in the specimens exposed under applied stress. Later work also demonstrated that SCG was observed in the hot-pressed material after oxidation under stress.[26–29] Depending on the type of test and the temperature, crack blunting or crack growth will occur in this material. The amount of SCG will depend on the level of oxidation, which again will depend on flaw shape and size, such that blunting would be preferred over growth for some material-test-temperature combinations. Some creep studies of sintered α-SiC have been performed,[29,30] and a creep exponent of one was found in bending. A number of creep studies have been performed on various types of siliconized SiC, and it was reported that there is competition between creep and SCG as described above.[31–35] The creep mechanism is characterized mostly by the formation of cavities at the silicon–silicon carbide interface, with the aid of high localized stresses and impurities in the silicon phase, and by cavity formation on the facets of large SiC grains which typically exist in this material. The creep properties of Si-SiC are strongly dependent on the amount of Si and its distribution in the microstructure.

2 Experimental procedure

2.1 Materials and procedures

The SCG properties of three materials are compared in this work. These are NT230 Si-SiC from Saint-Gobain Norton; β-SiC from Coors Ceramics Co.; and $SiCp/Al_2O_3$ from Du Pont Lanxide Composites Inc. NT230 SiC is a siliconized silicon carbide and contains ~ 8 vol% free silicon metal and some residual porosity ($\sim 2\%$); β-SiC is a sintered silicon carbide with a fine grain structure and high density. The $SiCp/Al_2O_3$, which is manufactured by the Lanxide Directed Metal Oxidation Process, contains 48 vol% SiCp, 38 vol% Al_2O_3, and 13 vol% Al-alloy. Some residual porosity ($\sim 1\%$) is also present in the material. The SiC ceramics were tested as machined while the $SiCp/Al_2O_3$ was reoxidized by the manufacturer after machining. The three materials were tested in four-point flexure at 1100 and 1400°C, using a hydraulic flexure testing system operating in load control. Fast-fracture tests were carried out at a loading rate of 45 N s^{-1}, resulting in a stressing rate of 37 MPa s^{-1} at all three temperatures (30 specimens at each temperature); specimen size was $3 \times 4 \times 50$ mm and inner and outer spans were 20 and

40 mm, respectively. Dynamic fatigue experiments were performed at 1100 and 1400°C in air at loading rates from 1·2 N s^{-1} to 0·00012 N s^{-1}, resulting in stressing rates of 1·0, 0·01, 0·001, and 0·0001 MPa s^{-1} (10 specimens at each condition). The purpose of the dynamic fatigue experiments was to determine if SCG existed in these materials. This experimental data was obtained to serve as a baseline for later studies of these materials in environments expected in advanced coal-burning combined-cycle systems.

2.2 Dynamic fatigue

The conventional approach for comparing the SCG behavior of various materials is to determine and compare the slow-crack growth parameter, n, as determined by the fracture mechanics model.[36,37] In this model, the subcritical crack velocity is commonly expressed empirically as a power function of the applied stress intensity factor, K_a, at the crack tip:

$$v = v_0\left(\frac{K_a}{K_{IC}}\right)^n$$

where v_0 and n are environmentally dependent constants, and K_{IC} is the critical stress intensity factor. The crack velocity exponent n is determined in the dynamic fatigue experiment by measuring the fracture stress as a function of stressing rate $\dot{\sigma}_a$:

$$\sigma_f^{n+1} = B(n+1)\sigma_i^{n-2}\dot{\sigma}_a$$

where σ_f is the fracture strength at the given stressing rate, σ_i is the inert (fast-fracture) strength, and:

$$B = \frac{2K_{IC}^2}{(n-2)v_0 Y^2}$$

with Y as a specimen/crack geometry factor.

2.3 Static fatigue

Static fatigue tests were performed in order to investigate the SCG to creep transition. Two types of flexural static test were conducted using the same four-point flexure fixtures as described above; a static load was applied for 300 h, or a static load was applied every 100 h in steps corresponding to 50 MPa up to a total of 500 h or to failure. Displacement was monitored during loading, and after the test permanent curvature was measured.

2.4 Fractographic investigation

Fractography is a necessary tool in assessing SCG behavior. If strength degradation is observed as a function of time, microscopy can aid in determining the mechanisms for the degradation, i.e. whether SCG or other strength-degrading mechanisms are operative. Fractography was performed by light optical and scanning electron microscopy (SEM) methods. The importance of performing fractography in experiments like these cannot be over estimated, as it is important to determine whether the fracture mode changes with time, temperature, environment, and crack velocities.[22,38]

3 Results and discussion

The fast-fracture strengths of the three materials are shown in Figs 1 and 2, for 1100 and 1400°C respectively. A summary of the strengths and Weibull parameters is given in Table 1, where the room temperature fast-fracture strengths have been included for comparison. The dynamic fatigue results for the three ceramics are shown in Figs 3 and 4, for 1100 and 1400°C respectively.

The Si-SiC exhibited a slight increase in the fast-fracture strength from room temperature to 1100°C, and then a significant drop in strength was observed at 1400°C. The Weibull modulus, m, for each of the three sets of 30 specimens ranged from 11, at room temperature, to 3, at 1400°C. As can be seen from Fig. 2, the strength values for the Si-SiC measured at 1400°C seemed to fall into two groups as indicated by the different symbols in the figure. Investigation of these two groups revealed two different fracture initiating flaws, pores or metal-rich areas, corresponding to two different production batches. The appropriate approach will therefore be to separate these strength data into two different exclusive flaw populations and perform the Weibull analysis accordingly. For a discussion of these results and their implications, see Breder (1995).[39] At 1100°C no strength reduction was observed as a function of stressing rate for the Si-SiC material, however, the scatter in the strength results was quite high. The strengths

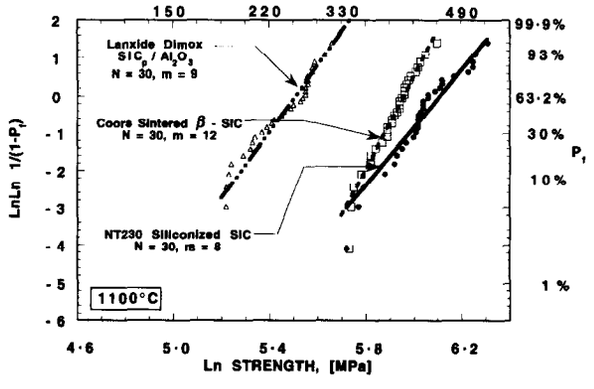

Fig. 1. Weibull graphs of fast-fracture strength for Si-SiC, β-SiC, and SiCp/Al_2O_3 measured at 1100°C.

measured at the slowest stressing rate (0·0001 MPa s^{-1}), at 1100°C, were consistently found to lie around 450 MPa, and typically required a time to failure of about 1250 h. In order to check if the specimens had undergone creep in that time, the load deflection curves were monitored and the specimens were inspected for permanent deflection after the test. At 1100°C no significant residual deflection was observed.

At 1400°C, a significant strength reduction was seen as a function of stressing rate for the Si-SiC ceramic. Also, more scatter was apparent in the strength data at the various stressing rates, a result of the batch-to-batch variation, as described above. This temperature is very close to the melting point of Si and it is likely that there were enough impurities present in the Si to lower the melting point below 1400°C, an assumption supported by the observation of metal beads on the surface of some of the specimens.[39] The total time to failure at the slowest stressing rate at 1400°C was approximately 400 h, and these specimens also showed essentially no permanent deflection; the strength calculations (elastic beam) were assumed to be valid. The SCG parameter, n, was calculated according to eqn (2) and found to be 15·5. This value is of the same order of magnitude as reported for hot-pressed SiC,[23–27] and lower than that for sintered SiC.[23,29] It is important to notice that this is a value of the SCG parameter which indicates that there will be a significant strength reduction over time, and this must be taken into account in the design of components of this material if used at this temperature.

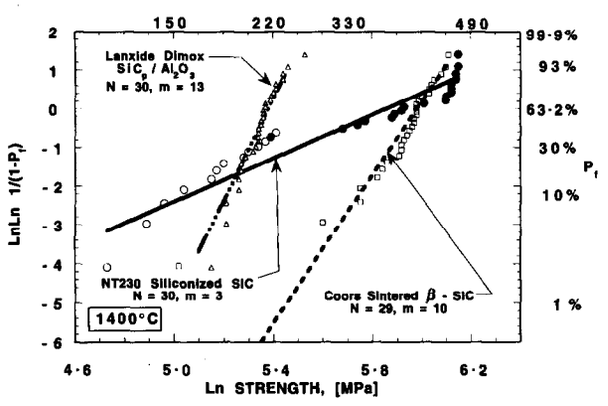

Fig. 2. Weibull graphs of fast-fracture strength for Si-SiC, β-SiC, and SiCp/Al_2O_3 measured at 1400°C. The open and closed symbols for Si-SiC refer to two different material batches.

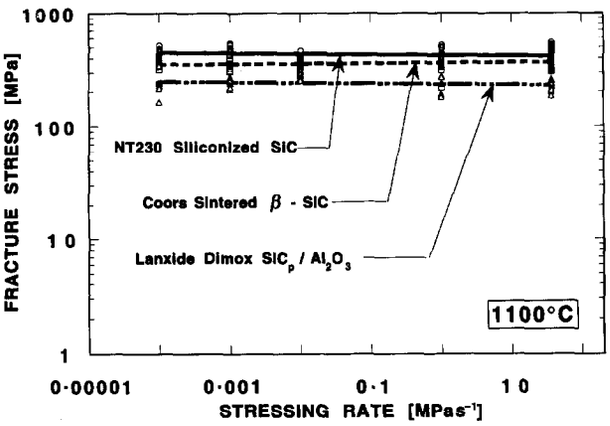

Fig. 3. Strength as a function of stressing rate for Si-SiC, β-SiC, and SiCp/Al_2O_3 measured at 1100°C.

Figures 1 through 4 show that the strength of Coors β-SiC was remarkably unaffected by temperature and stressing rate. A slight strength reduction as a function of time was seen at 1100°C, but the 8% drop in strength at a time to failure of more than 1000 h (stressing rate of 10^{-4} MPa s^{-1}) will result in an n value of 250, too high to develop a significant amount of SCG. At 1400°C, the strength level for the β-SiC remained almost unchanged at all stressing rates.

The results shown in Figs 1 through 4 indicate that there was no significant strength reduction as a function of applied stressing rate at any temperature for the SiCp/Al_2O_3. However, it is important to note that this material could only be tested up to stressing rates of 0·01 MPa s^{-1} at 1400°C. At the slower stressing rates, creep became so pronounced that the four-point flexure fixtures could no longer accommodate the specimens and, of course, the elastic beam assumption was violated. Also, at the 0·01 MPa s^{-1} stressing rate, the creep was measurable; and the strength values calculated according to beam theory therefore overestimate the strength of the SiCp/Al_2O_3 under these conditions.

Table 1. Summary of fast-fracture strength and Weibull parameters for three ceramics

	No. of specimens	*Weibull modulus m*	*Weibull characteristic strength S_0 (MPa)*	*Average strength (MPa)*
β-SiC RT	30	12	390	374
β-SiC 1100°C	30	12	388	374
β-SiC 1400°C	29	10	397	376
Si-SiC RT	30	11	404	386
Si-SiC 1100°C	30	8	450	424
Si-SiC 1400°C	30	3	348	308
SiCp/Al_2O_3 RT	30	10	435	414
SiCp/Al_2O_3 1100°C	30	9	246	233
SiCp/Al_2O_3 1400°C	30	13	217	210

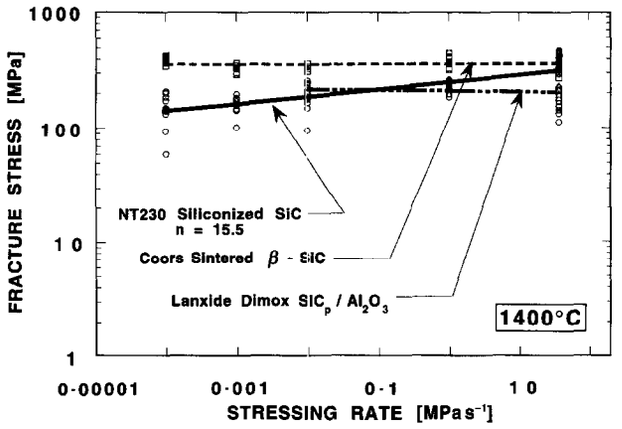

Fig. 4. Strength as a function of stressing rate for Si-SiC, and β-SiCp/Al_2O_3 measured at 1400°C.

The creep properties of this SiCp/Al_2O_3 composite were investigated by performing static and stepped tests in four point flexure. At 1100°C very little permanent deflection was observed, and static testing resulted in increased permanent deflection at 1200°C. Static measurements at 1260°C showed an increasing creep rate, and at 1300 and 1400°C the creep rates were quite high. All these temperatures were well above the melting point of Al-alloys, but only at the highest temperature would molten metal be apparent on the fracture surface. In no case did molten metal seep out through the surface oxide layer. A thorough description of the flexural creep measurements for this material is given elsewhere.[40]

For Si-SiC, fractography provided further insight into the SCG results. At 1100°C, for all stressing rates, the fracture surfaces all showed the characteristics of fast fracture. The fracture-initiating flaws were predominantly pores located near the tensile surface. A typical example is shown in Fig. 5, for a specimen tested at 1100°C, at 0·0001 MPa s^{-1}. At 1400°C for the faster stressing rates, the failure mode for the Si-SiC was of the fast-fracture type with pores or Si-rich areas acting as fracture initiation points. At the two slowest stressing rates (0·0001 MPa s^{-1} and 0·001 MPa s^{-1}) strength degradation was observed and the fracture surfaces showed evidence of damage zones. These damage zones seemed from the SEM observations to be created from areas which were rich in Si-alloy (see Fig. 6 for a typical example).

Fractography of the β-SiC material showed that the failure mode remained unchanged with temperatures and stressing rates. The majority of specimens (for all conditions) failed from pores of the type shown in Fig. 7.

For the SiCp/Al_2O_3 composite, fractography showed that the majority of the specimens failed from metal inclusions of the type shown in Fig. 8. At 1400°C, the inclusions tended to be larger, and at the slower stressing rates, the specimens failed from creep damage as shown in Fig. 9. The creep damage differed from SCG zones in the existenceof an area with a rough surface and multiple cracks and ridges which finally coalesced to cause failure. Fractographic investigation of the specimens fractured under various creeping conditions showed this type of creep damage. Under none of the test conditions was any damage typical of SCG observed, i.e. damage zones which would consist of growth of cracks around the metal-rich inclusions which were the fast-fracture failure origins. The implication is that this SiCp/Al_2O_3 composite does not exhibit SCG under the present conditions, but undergoes a transition from a fast-fracture failure mode at 1100°C (at slow stressing rates) to creep failure at 1260°C and 1400°C, at intermediate stressing rates and fast stressing rates, respectively.

4 Conclusions

The room-temperature strengths of the three ceramics studied here were very comparable, at about 400 MPa. This strength level is assumed to be sufficient for the present application; i.e. for transport and assembly of ceramic heat exchangers. In situ, it is not expected that heat exchanger tubes would experience stresses at such high levels, unless excursions from normal operating conditions are experienced.

The Si-SiC ceramic did not exhibit SCG at 1100°C, but at 1400°C, strength degradation was observed as a function of stressing rate, and the n value was found to be ~15·5 at 1400°C. This is a significantly low number so that strength degradation over time must be accounted for in component design.

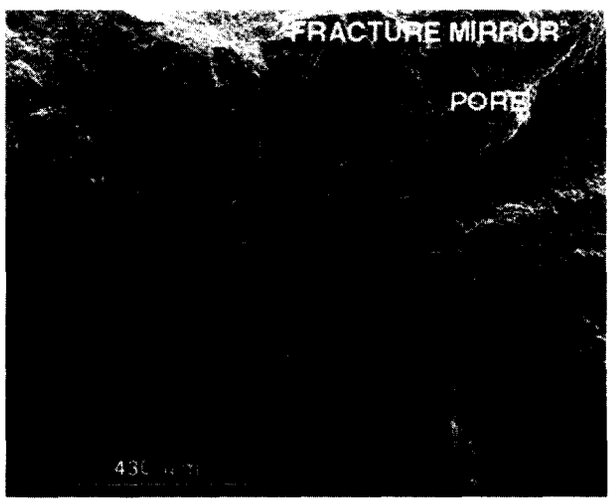

Fig. 5. Typical fracture-initiating flaw in Si-SiC measured in fast-fracture at 1400°C.

The dynamic fatigue experiments showed that Coors β-SiC exhibited no SCG over the temperature and stressing rate regime used in these experiments. Earlier studies on sintered SiC had shown that some SCG may occur at higher temperatures, but the current material exhibited no such behavior. It is important to note that the present experiments also range over considerably longer testing times (slower stressing rates) than were employed in most of the results cited in the literature. It would therefore seem to be a sound conclusion that this type of SiC does not exhibit SCG up to 1400°C.

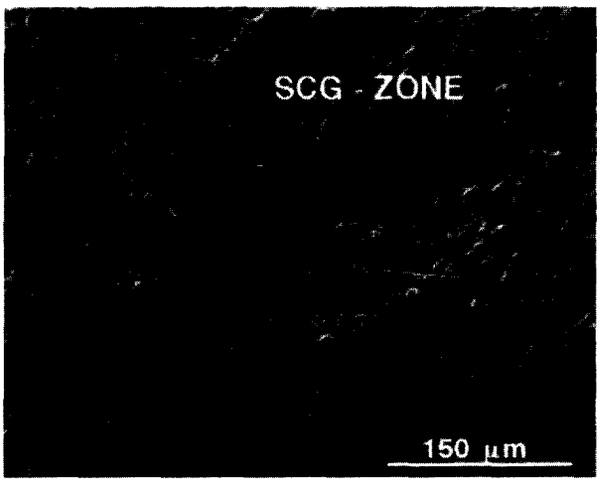

Fig. 6. Slow-crack growth region in SiSiC measured at 1400°C at a stressing rate of 0·0001 MPa s^{-1}.

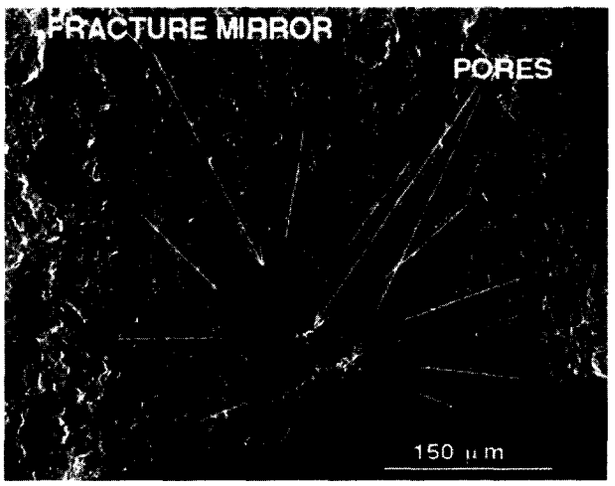

Fig. 7. Typical fracture-initiating flaw in β-SiC measured in fast-fracture at 1400°C.

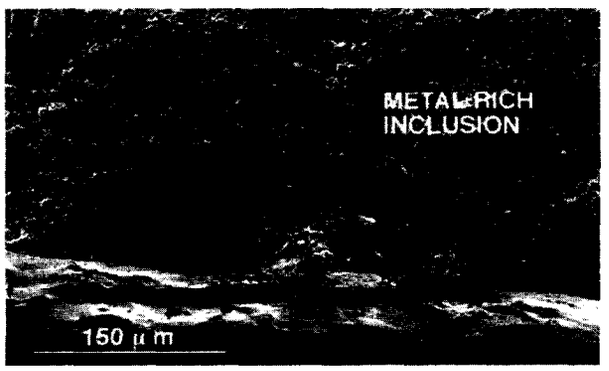

Fig. 8. Typical fracture initiating flaw in $SiCp/Al_2O_3$ measured in fast-fracture at room temperature. The tensile surface in the lower part of the figure is smooth due to the reoxidation procedure the specimens underwent prior to testing.

The $SiCp/Al_2O_3$ composite did not exhibit SCG at 1100 or 1400°C. However, at 1400°C, creep became the dominating failure mechanism at stressing rates of 0·01 MPa s^{-1} and less. At 0·001 MPa s^{-1}, creep became sufficient that the specimens deformed and reached the bottom of the fixture before they fractured. At 0·01 MPa s^{-1}, the specimens were fractured at a load comparable to the fast-fracture load; however, the specimens had undergone considerable creep deformation, and the resulting strength calculated from elastic beam theory was therefore overestimated. Consequently, the $SiCp/Al_2O_3$ composite experienced some strength reduction as a function of stressing rate, but this was primarily due to creep rather than SCG, as was confirmed by the fractographic investigation. At 1100°C, creep was much less important, although some permanent deflection was observed after long testing times at this temperature.

The failure modes were investigated by optical microscopy and SEM. The observations on fracture-initiation sites are consistent with the strength measurements. Si-SiC experienced failure from pores at room temperature. At elevated temperature, fast-fracture failures were from pores or metal-rich areas, dependent on the batch of material. At 1100°C, the failures at the various stressing rates were consistent with no strength loss; i.e.

Fig. 9. Creep damage in $SiCp/Al_2O_3$ measured at 0·01MPa s^{-1} at 1400°C.

failures were initiated from pores or metal-rich areas, as in the case of fast-fracture. At 1400°C the failure modes changed as a reduction in strength was observed. At stressing rates of 0·001 and 0·0001 MPa s^{-1}, SCG zones which had originated from metal-rich areas were observed. Coors β-SiC failed from pores at all temperatures and stressing rates, consistent with the very uniform strength values and Weibull moduli. SiCp/Al_2O_3 failed from metal-rich areas at lower temperatures and faster stressing rates, but the fracture mode changed to creep failure for the slower stressing rates at 1400°C. The difference between the SCG zones observed in Si-SiC and creep failure observed in SiCp/Al_2O_3 is that the SCG zone was localized and had clearly grown out from a specific flaw, while the fracture surface in the crept specimens showed a larger damage area spread out over the tensile zone and contained numerous small cracks. Under none of the combinations of stress, stressing rate and temperature were any indications of SCG found in this material. It is therefore concluded that the SiCp/Al_2O_3 undergoes a transition from fast-fracture to creep failure without undergoing SCG.

The different behavior observed for these three ceramics has important implications for the approach to use in the design of ceramic components. For the β-SiC material, design can be performed using fast-fracture and reliability concepts, while for the Si-SiC different design data will have to be used for different temperature regimes. At 1400°C, not only does the high variability of the material need to be taken into account, but also the shortened time to failure due to SCG. For the SiCp/Al_2O_3 composite, a design against creep failure must be applied, noting especially that creep becomes more pronounced at higher temperatures.

Acknowledgement

Research sponsored by the U.S. Department of Energy, Office of Fossil Energy, Pittsburgh Energy Technology Center, Advanced Combustion Technology Program, DOE/FE AA 20 10 00 0, under contract DE-AC05-96OR22464 with Lockheed Martin Energy Research Corporation.

References

1. Klara, J. M., HIPPS: beyond state-of-the-art Part 1. *Power Eng.*, 1993, **12**, 37–39.
2. Klara, J. M., HIPPS can compete with conventional PC systems. Part 2. *Power Eng.*, 1994, **1**, 33–36.
3. Seery, D. J. et al., Combustion 2000: burning coal in the twenty-first century. In *Proceedings from the Ninth Annual Coal Preparation, Utilization, and Environmental Control Contractors Conference, Pittsburgh, Pa, July, 1993*, U.S. DOE, Pittsburgh, 1993, pp. 356–363.
4. Shenker, J., Development of a high-performance coal-fired power generating system with a pyrolysis gas and char-fired high temperature furnace. In *Proceedings from the Ninth Annual Coal Preparation, Utilization, and Environmental Control Contractors Conference, Pittsburgh, Pa., July, 1993*. US DOE, Pittsburgh, 1993, pp. 349–355.
5. Kotchick, D. M., Coombs, M. G. and Bakker, W. T., Development of a high pressure ceramic heat exchanger. In *Advances in Ceramics*, Vol. 14, *Ceramics in Heat Exchangers*, eds B. D. Foster and J. B. Patton, American Ceramic Society, Columbus, Ohio, 1985, pp. 227–241.
6. Ward, M. E., Solomon, N. G., Gulden, M. E. and Smelzer, C. E., *Development of a Ceramic Tube Heat Exchanger with Relaxing Joint*. DOE Contract No. FE-77-C-01-2556 with Solar Turbines International, June 1980.
7. Ferber, M. K. and Tennery, V. J., Evaluation of tubular ceramic heat exchanger materials in basic coal ash from coal-oil-mixture combustion. *Ceram. Bull.*, 1984, **63**(7), 898.
8. Ferber, M. K. and Tennery, V. J., Evaluation of tubular ceramic heat exchanger materials in acidic coal ash from coal-oil-mixture combustion. *Ceram. Bull.*, 1983, **62**(2), 236.
9. Ferber, M. K., Ogle, J., Tennery, V. J. and Henson, T. Characterization of corrosion mechanisms occurring in a sintered SiC exposed to basic coal slags. *Journal of Am. Ceram. Soc.*, 1985, **68**(4), 191.
10. Becher, P. F., Strength degradation in SiC and Si_3N_4 ceramics by exposure to coal slags at high temperatures. *Journal of Mater. Sci.*, 1984, **19**, 2805.
11. Easler, T. E., *Corrosion Behavior and Mechanical Properties of Silicon Carbide Exposed to Coal Gasification Environment*. Report ANL/FE-84-21, Argonne National Laboratory, June 1985.
12. Easler, T. E., *Effects of Coal Gasification Environments on Corrosion Behavior and Mechanical Properties of Siliconized Silicon Carbide*. Report ANL/FE-85-6, Argonne National Laboratory, 1985.
13. Easler, T. E., *Influence of Oxidizing and Reducing Environments on Coal-Slag-Induced Corrosion of Silicon Carbide Ceramics*. Report ANL/FE-85-11, Argonne National Laboratory, 1985.
14. Easler, T. E., *Comparisons of Results of 200 – and 500-h Exposures of Silicon Carbide to a Slagging Coal Gasification Environment*. Report ANL/FE-85-13, Argonne National Laboratory, 1986.
15. Kern, W. A., Tressler, R. E. and McNallan, M. J., Durability of SiC/Al_2O_3 Composites in Contact with Sodium Silicate. In *Center for Advanced Materials*, Vol. 6, No. 1, Pennsylvania State University Press, University Park, Pa., 1992.
16. Johnson, W. B. and Landini, D., DuPont Lanxide Composites Inc., (Pers. comm. May 1993).
17. Strobel, T. M., Hurley, J. P., Breder, K. and Holowczak, J. E., Coal-slag corrosion and strength degradation of silicon carbide-alumina composites. *Ceram. Eng. Sci. Proc.*, 1994, **14**(4), 579–586.
18. Strobel, T. M. and Hurley, J. H., Coal-slag corrosion of SiC-based ceramics in a combustion environment. To be published in the proceedings of the American Ceramic Society Pacific RIM Meeting, held in November 1993.
19. Breder, K., Tennery, V. J., Strobel, T. M., Hurley, J. P. and Holowczak, J. E., Strength measurements of monolithic SiC and Al_2O_3/SiC composites after exposure to coal slag. *Journal of Am. Cer. Soc.*, 1995, **78**(10) 2837–2840.
20. Trantina, G. G. and Johnson, C. A., Subcritical crack growth in boron-doped SiC. *Journal of Am. Ceram. Soc.*, 1975, **58**(7–8), 344–345.
21. Evans, A. G., Lange, F. F. Crack propagation and fracture in silicon carbide. *Journal of Mater. Sci.*, 1975, **10**(10), 1659–1664.

22. Quinn, G. D. and Katz, R. N., Time dependent high-temperature strength of sintered α-SiC. *Journal of Am. Ceram. Soc.*, 1980, **63**(1–2), 117–119.
23. McHenry, K. D. and Tressler, R. E., Fracture toughness and high-temperature slow crack growth in SiC. *Journal of Am. Ceram. Soc.*, 1980, **63**(3-4), 1152–1156.
24. McHenry, K. D. and Tressler, R. E., High temperature dynamic fatigue of hot-pressed SiC and sintered α-SiC. *Am. Ceram. Soc. Bulle*, 1980, **59**(4), 459–461.
25. Easler, T. E., Bradt, R. C. and Tressler, R. E., Strength distributions of SiC ceramics after oxidation and oxidation under load. *Journal of Am. Ceram. Soc.*, 1981, **64**(12), 731–734.
26. Minford, E. J., Costello, J. A., Tsong, I. S. and Tressler, R. E., Oxidation effects on crack growth and blunting in SiC ceramics. In *Fracture Mechanics of Ceramics*, Vol. 6, eds R. C. Bradt, A. G. Evans, D. P. H. Hasselman, and F. F. Lange, Plenum Press, New York, 1983, pp. 511–522.
27. Larsen, D. C., Adams, J. W., Bortz, S. A. and Ruh, R., Evidence of strength degradation by subcritical crack growth in Si_3N_4 and SiC. In *Fracture Mechanics of Ceramics*, Vol. 6, eds R. C. Bradt, A. G. Evans, D. P. H. Hasselman, and F. F. Lange, Plenum Press, New York, 1983, pp. 571–585.
28. Govila, R. K., Phenomenology of fracture in sintered alpha silicon carbide. *Journal of Mater. Sci.*, 1984, **19**, 2111–2120.
29. McCullum, D. E., Hecht, N. L., Chuck, L. and Goodrich, S. M., Summary of results of the effects of environment on mechanical behavior of high-performance ceramics. *Ceram. Eng. Sci. Proc.*, 1991, **12**(9-10), 1886–1913.
30. Lin, H. T. and Becher, P. F., Fracture behavior of toughened ceramics. ORNL Report W.B.S. Element 3.2.1.3., bimonthly report April 1991.
31. Carter, C. H. Jr., Davis, R. F., Bentley, J. Kinetics mechanisms of high temperature creep in silicon carbide: I. reaction-bonded. *Journal of Am. Ceram. Soc.*, 1984, **67**(11), 409–417.
32. Chuang, T-J. and Wiederhorn, S. M.Damage-enhanced creep in a siliconized silicon carbide: mechanics of deformation. *Journal of Am. Ceram. Soc.*, 1988, **71**(7), 595–601.
33. Wiederhorn, S. M., Roberts, D. E., Chuang, T-J. and Chuck, L., Damage-enhanced creep in a siliconized silicon carbide: phenomenology. *Journal of Am. Ceram. Soc.*, 1988, **71**(7), 602–608.
34. Carroll, D. F. and Tressler, R. E., Accumulation of creep damage in a siliconized silicon carbide. *Journal of Am. Ceram. Soc.*, 1988, **71**(6), 472–477.
35. Carroll, D. F. and Tressler, R. E., Effect of creep damage on the tensile creep behavior of a siliconized silicon carbide. *Journal of Am. Ceram. Soc.*, 1989, **72**(1), 49–53.
36. Evans, A. G., A method for evaluating the time-dependent failure characteristics of brittle materials and its application to polycrystalline alumina. *Journal of Mater. Sci.*, 1972, **7**, 1137–1146.
37. Ritter, J. E., Engineering design and failure of brittle materials. In *Fracture Mechanics of Ceramics*, Vol. 4, eds R. C. Bradt, D. P. H. Hasselman, and F. F. Lange, Plenum Press, New York, 1983, pp. 667–686.
38. Zeng, K., Breder, K. and Rowcliffe, D. J., Comparison of slow crack growth behavior in alumina and SiC — whisker-reinforced alumina. *Journal of Am. Ceram. Soc.*, 1993, **76**(7), 1673–1680.
39. Breder, K., Time-dependent strength degradation of a siliconized silicon carbide determined by dynamic fatigue. *Journal of Am. Cer. Soc.*, 1995, **78**(10), 2680–2684.
40. Lin, H. T. and Breder, K., Creep deformation in an alumina-SiC composite produced via a directed metal oxidation process. *Journal of Am. Cer. Soc.*, 1996, **79**(8), 2218–2220.